

A 140,000-year continental climate reconstruction from two European pollen records

J. Guiot, A. Pons, J. L. de Beaulieu & M. Reille

Laboratoire de Botanique historique et Palynologie, URA CNRS D1152, Faculté des Sciences et Techniques St-Jérôme, 13397 Marseille Cedex, France

The dramatic and cyclic changes that have characterized the Earth's climate throughout the Quaternary may be illustrated by developments during the last such cycle which took place over the past 140,000 years. Quantitative reconstruction of the continental climate over this period improves the correlation between marine and land records and emphasizes the role of post-temperate forested episodes at the beginning of ice-sheet formation.

IN 1971, Imbrie and Kipp¹ used foraminiferal data obtained from deep-sea cores in palaeoclimate reconstruction. Since then, different multivariate techniques have been used to calculate palaeoclimate parameters from fossil biological data. For continental records, pollen analysis provides the most reliable data². Pollen is deposited as 'pollen rain' which can be characterized by a percentage representation of its components, the so-called 'pollen spectrum'. This provides a reliable reflection of regional vegetation³, and hence of regional climate. Past climates can therefore be established from the pollen content of sediments favourable to pollen preservation. Quantitative analysis of such records has until now provided palaeoclimate reconstructions for relatively short periods^{4,5}. Here we present the results of applying an improved and simplified method⁶, using pollen-stratigraphic records from La Grande Pile⁷ and Les Echets⁸, in eastern France, each containing a sediment sequence for the past 140,000 yr.

The results agree well with the palaeoclimate information derived from marine isotope data and emphasize the role of forested periods before glacial stadials as important episodes of ice-sheet formation. We also show that the arboreal pollen sum, often used by palaeoclimatologists as an index of continental temperature, is inadequate for this purpose.

Methods

We assume that different climates and their corresponding vegetation types and pollen spectra, which have succeeded each other through time in the study area, can be found today in similar, analogous forms. It follows, therefore, that in order for climates to be represented that are quite different from those at the studied locality today, a very extensive study area is required to provide a wide range of analogues. We therefore first establish representative modern pollen spectra from a large area with wide variations in present-day climate and vegetation; then we define precise climate data for all the sites from which pollen spectra are obtained and identify modern spectra that are most similar to each fossil spectrum. Finally we use modern climate parameters corresponding to the best analogues to infer past climatic conditions.

There are three main problems: The climate requirements of modern plants may be different from those in the past; the range of past climatic conditions may not be fully represented today; and past and present human activity has disturbed the vegeta-

tion/climate, and hence the pollen/climate relationships in the modern pollen data set.

It is unlikely, however, that any major evolutionary changes in trees or herbs (considered here at the genus level) have occurred over the past 140,000 yr. The second problem can be overcome to an extent by using the greatest variety of modern spectra available. We try to minimize anthropogenic effects by using a method for identifying the best analogue spectra; the percentages corresponding to each taxon have been attributed a 'loading factor' which expresses the role it has played at the site throughout the period covered by the reconstruction.

Data

The modern data, covering Europe, North Africa and Siberia, are represented by 227 spectra selected to represent a wide variety of vegetation types and climates. The 182 spectra described by Guiot⁶ are complemented by new data from Morocco, Tunisia, Italy and Corsica, so that a total of 52 taxa could be used.

Annual temperatures and precipitation were interpolated for localities from which the spectra were collected⁶. Among the taxa of fossil spectra, only the 52 taxa used in the modern spectra were considered.

The Grande Pile record (47°44' N, 6°30'14" E, 330 m above sea level) is from three cores⁷: 'Grande Pile 1' for the Holocene (depth: 55–320 cm), 'Grande Pile XIV' for the end of the last glacial (depth: 452–1,193 cm) and 'Grande Pile X' for older periods (depth: 1,243–1,865 cm). We analysed 268 pollen spectra and as "the miscellaneous and varying content of the pollen spectra from the section 1,170 cm–1,240 cm explains the hypothesis proposed by Gruber (1979) that they include quite a number of rebedded pollen, which deprives them of all botanical and hence climatical significance"⁸, we have neglected this particular section.

The Echets record (45°48'30" N, 4°55'20" E, 267 m above sea level) corresponding to the 39-m core of Les Echets G⁸, yielded 573 spectra (out of the 800 analysed). It was shown⁸ that the spectra from the episodes 'Melisey I' and 'Melisey II' were contaminated by reworked arboreal pollen (AP) from earlier temperate deposits, and so for these episodes the mesic AP frequencies were limited to mean values recorded at La Grande Pile for the same periods. As the Les Echets record does not include the Holocene, data for this period are derived from Hières-sur-Amby, 30 km to the south-east but at the same elevation⁹.

Results

First, we produced a time analysis of each spectra sequence to calculate how each taxon should be weighted as a climate signal. The modern ecological correlation between each taxon and climate cannot be used because of anthropogenic effects. When several well dated contemporaneous sequences are available, information that is common to all of them (mostly of a palaeobioclimatic nature) can be used⁶. In the present case, only the information conveyed from one level to another can be taken into account (Fig. 1a). However, such information is contaminated by noise from the local site peculiarities and (for about

the past 1,000 yr) human activity. Moreover the vegetation at any time is a function not only of the climate at that time but also of previous vegetation and climate.

Now, successive eigenvectors represent different parts of the autocorrelation (Fig. 1a), and therefore only the first eigenvector—in which climate is necessarily dominant—is retained; the others—in which noise is assumed to be dominant—are removed. Moreover, this first eigenvector maximizes autocorrelations and hence the persisting action of climate on vegetation.

The weight attributed to each taxon in the first eigenvector defines its particular role in the biological expression of the climate changes that occurred during the period concerned, and is termed the palaeobioclimatic operator (PBO). When applied to the fossil sequence, it provides a times series which can be considered as the best possible climate profile of vegetation changes.

There is a close correlation between the time series of La Grande Pile and Les Echets (Fig. 2), indicating that the operator, although derived from an autocorrelation analysis made at a single site, has a regional and therefore a climate value. This shows *a posteriori* the effective removal of any noise.

Figure 2 also shows the fluctuation of the AP sum often used by non-botanists as a palynological climate index. Note that the correlation between the AP sum at La Grande Pile and Les Echets, especially in relation to amplitude, is not as clear as that between the PBOs. In addition, comparison between the time series and the AP at each site (correlation coefficient $r = 0.87$ at La Grande Pile and 0.85 at Les Echets) shows two main differences: the PBO increases later and decreases earlier than the AP sum; and amplitude variations in the PBO are smaller

FIG. 1 The reconstruction method may be summarized as follows: a, The transfer of the climatic information from one level to the other is estimated by the first-order multiple autocorrelation matrix A_1 between the m taxa, computed on the n fossil spectra. The element (j, l) of A_1 is the cross-correlation coefficient between taxon j and l :

$$r_{jl} = \frac{1}{n} \left[\sum_{t=2}^n \frac{f_{jt} - \bar{f}_j f_{(t-1)l} - \bar{f}_l}{S f_j S f_l} \right],$$

where f_{jt} represents the frequency (in percentages multiplied by 10) of taxon j in fossil spectrum t , the upper-bar represents the mean calculated across the fossil sequence and S is the standard deviation. As in principal component analysis—with a specific treatment to take into account its asymmetric character— A_1 is reduced to a few eigenvectors. The first eigenvector explains ~70% of the sum of squared autocorrelations (72% for La Grande Pile and 69% for Les Echets). The second eigenvector (and the succeeding ones), explaining <10% of this sum, are not retained. The weights w_j of each taxon in the first eigenvector (called PBO) are used in the second step, and also to provide the time series of the PBO (see Fig. 2): $b_t = \sum_{j=1}^m w_j (f_{jt} - \bar{f}_j) / S f_j$, $t = 1, \dots, n$. b, A weighted euclidian distance operator, integrating the PBO, is used to measure the similarity between fossil and modern pollen spectra and to identify the best-fit analogues for the fossil spectra: $d_{it}^2 = \sum_{j=1}^m w_j^2 (\ln(f_{jt} + 1) - \ln(f_{it} + 1))^2$, where t is the index of fossil spectra, i for modern spectra, and w_j is the PBO loading affected to taxon j . This set of k most similar modern spectra is denoted $(P_{t_1}, \dots, P_{t_k})$. However, because the modern data set may not include an exact analogue for each fossil spectrum, the single best-fit modern spectrum may not be appropriate. Instead, we prefer a Monte Carlo simulation of the data, whereby k spectra are randomly extracted with replacement from the k selected spectra, and the best-fit spectrum from that group is obtained. This is repeated s times, providing s analogues from which confidence intervals are calculated. c, The estimated past climate (analogue climate R_t) for a given analogue, indexed by k , from which the distance is d_{ik} is given by

$$R_t = \left(\sum_{k=1}^s C_k / d_{ik}^2 \right) / \left(\sum_{k=1}^s d_{ik}^{-2} \right).$$

The lower and upper limits of this mean estimate are

$$\begin{aligned} -R_t &= R_t - \sqrt{\left(\sum_{k=1}^s C_k^2 / d_{ik}^2 \right) / \left(\sum_{k=1}^s d_{ik}^{-2} \right)} - R_t \\ +R_t &= R_t + \sqrt{\left(\sum_{k=1}^s C_k^2 / d_{ik}^2 \right) / \left(\sum_{k=1}^s d_{ik}^{-2} \right)} - R_t^2. \end{aligned}$$

The probability covering the interval $[-R_t, +R_t]$ is defined by the proportion of modern analogous climate C_k accounted for within the range of s values.

than those in the AP during episodes of generally low forest cover.

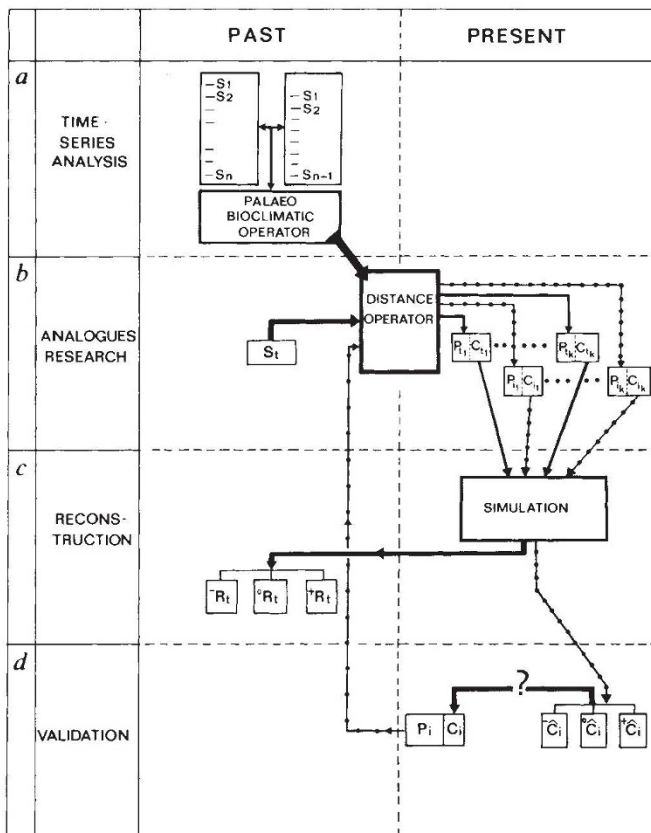
These differences arise because in the AP sum the pollen frequencies of all arboreal taxa are weighted equally whereas in the PBO the percentage of each tree taxon is weighted by its component weighting. For *Pinus* and *Betula*, this weighting may be very different from that of the other trees and close to the coefficient of non-arboreal taxa.

Figure 2 also shows that the variations in the PBO time series correspond more closely than do the AP curves to the oxygen isotope stages defined by Emiliani¹⁰ and Shackleton¹¹, represented by the stacked and smoothed record in the SPECMAP timescale¹².

We next look for analogues. A weighted euclidian distance ('distance operator'), in which the PBO provides a weighting for all pollen frequencies, is used to measure the similarity between ancient and modern spectra, thus enabling us to identify the best analogues for each fossil spectrum.

We then reconstruct palaeoclimate on the basis of the climatic characteristics of the best analogues. A Monte Carlo technique (Fig. 1b) enables us to derive a climate estimate with a confidence level (Fig. 1c) of about 70%. The confidence intervals average 180 mm and 2.1 °C (Table 1). These intervals are asymmetric and slightly larger for Les Echets.

Finally, we investigate both the validity of using a PBO and our method as a whole. We reconstruct climate parameters from modern pollen spectra for which values are known (Fig. 1d). The modern spectra are dealt with in the same manner as the fossil ones, and the reconstructed climatic parameters are compared to actual data (Table 1). The estimates correlate well (0.73 on average). The confidence intervals are slightly narrower than



This interval enables one to appreciate the quality of the analogues. This simulation procedure replaces the more complicated Kalman filtering previously used⁶. d, We use the entire procedure described in b and c, with index i replacing index t . The modern climate triplet $[C_i, \hat{C}_i, +\hat{C}_i]$ estimated in this way is compared with actual climatic parameters C_i (see Table 1: modern data column).

TABLE 1 Validation statistics of the reconstructions

		Fossil reconstructions		Modern reconstructions	
		Precip. (mm)	T (°C)	Precip. (mm)	T (°C)
Grande Pile	\bar{R} ME	173	2.1	138	1.8
	$+\bar{R}$ ME	183	1.8	178	1.7
	Cor	—	—	0.77	0.70
Echets	\bar{R} ME	156	2.2	141	1.6
	$+\bar{R}$ ME	198	2.4	164	1.8
	Cor	—	—	0.75	0.71

Cor is the correlation between estimated and actual data, \bar{R} ME is the mean upper standard deviation associated to the estimates ($+\bar{R}$ — \bar{R} in Fig. 1c), \bar{R} ME is the lower standard deviation (\bar{R} — $-\bar{R}$ in Fig. 1c). These statistics are calculated on the fossil data and on the modern data. In this last case R must be replaced by C (see Fig. 1d).

those computed on fossil data (155 mm and 1.7 °C on average) and have a higher confidence level (>90%). Such good agreement is particularly valuable as the modern estimates are based upon coefficients calculated solely from the fossil data.

The confidence interval mean is larger than that of other reconstructions (13, for example) based upon assumptions of a gaussian distribution and homogeneity between modern and fossil data. As these assumptions are never exactly satisfied, a more appropriate method, including a simulation approach, is used. Such a method provides less optimistic but more realistic confidence intervals. Note, however, that a part of the confidence interval reflects the variability of the calibration data set, so that the cold and dry periods have larger confidence intervals than the warm and/or humid ones. This suggests that the major weakness in our reference data set is a relative lack of cold and dry analogues, which of course it is difficult to compensate for, during the present temperate period.

Discussion

The reconstructions are obtained as a function of depth. To facilitate comparison with reconstructions from deep-sea cores,

the results are presented on a timescale (Fig. 3). The most important events before 30,000 yr BP are dated on the basis of the widely accepted isotopic chronology¹², whereas ^{14}C ages^{8,14} are used to date events after 30,000 yr BP (Fig. 2). Intermediate dates are linearly interpolated with steps of 1,000 yr.

We are aware that this procedure does not ensure the independence of our chronology with respect to that of the isotopic stratigraphy. But the succession—if not the chronology—of the climate phases shown by the pollen record is independent, and so are the reconstructed values even though the variation in time is, of course, derived from isotopic records.

The temperature and precipitation curves obtained at both sites agree well. The Holocene and the last interglacial (Eemian) appear clearly as the two warm and humid episodes which followed a complex period marked by significant rises in temperature and precipitation.

A temperature drop, which can be seen during the latter half of the Eemian and is clearly reflected in the vegetation changes, precedes a moisture maximum.

In agreement with botanical evidence, we find that a clear succession of two relatively warm and humid periods occurred after the Eemian. The first, the St-Germain I interstadial, appears as a climatically complex period because at both sites it is interrupted by relatively cold and humid short episodes and the latter half of this period is characterized by a precipitation maximum following a marked fall in temperature.

We found the two periods following the Eemian and the St-Germain I interstadial (the Melisey I and the Melisey II stadials, respectively) to be cold and dry, as expected.

For the second temperate period (the St-Germain II interstadial), we find warm and humid conditions overall, but with a tendency for low temperatures and high precipitation towards the end of the period.

The following period, the Lower Würmian Pleniglacial, was initially humid and cold, then very cold and very dry, as were the 'late Eemian-Melisey I' and the 'late St-Germain I-Melisey II' periods.

The Middle Würm then followed, a dry and cold period but far less severe than the previous stadials. At Les Echets, two

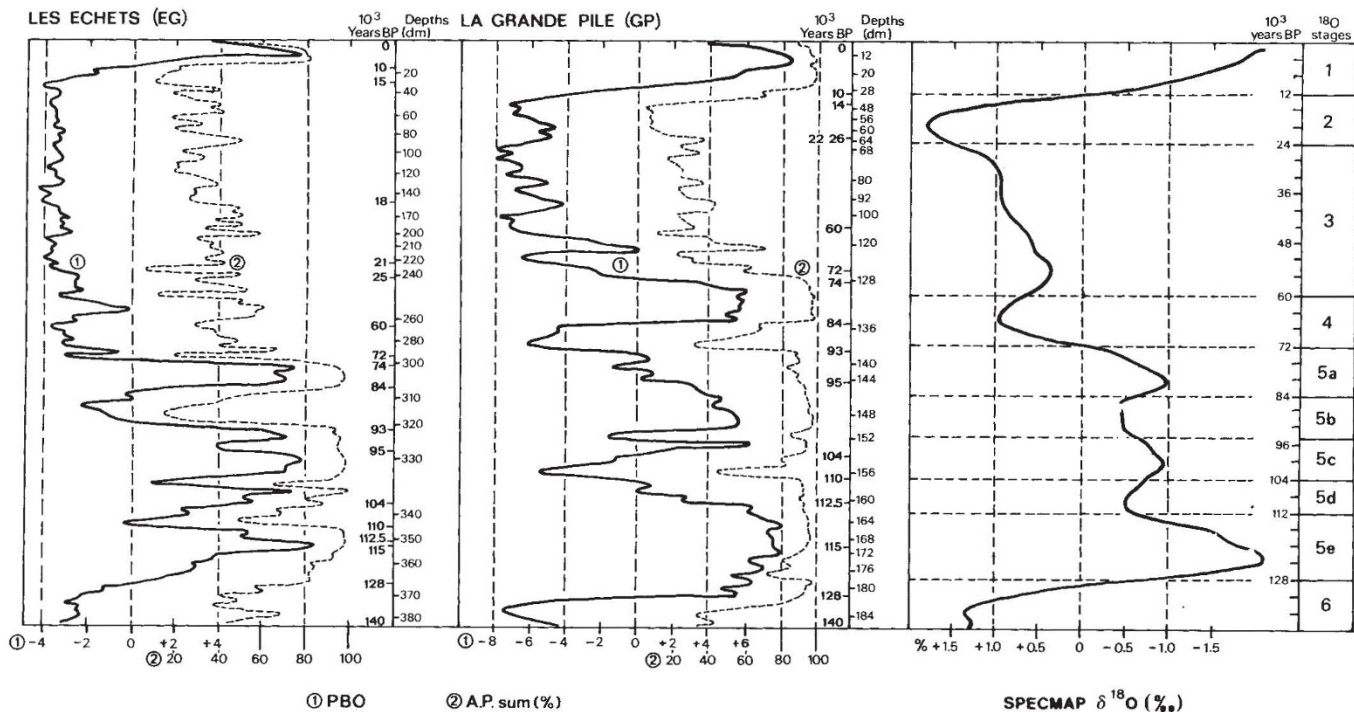


FIG. 2 The palaeobioclimatic operator time series, and the arboreal pollen (AP) sum (%) for Les Echets and La Grande Pile. These series are compared with the stacked, smoothed oxygen isotope record as a function of age using

the SPECMAP scale¹². The vertical axis is linearly related to the spectra numbers. Estimated ages are given with regard to the depths.

short temperate episodes comprised a rather cool middle phase, and at La Grande Pile we found the same division into two relatively temperate episodes with an intermediate cooler one. These results support the case for a threefold division of the Middle Würm, as suggested by European Atlantic micro-palaeontological data¹⁵ and insolation curves¹⁶. These results, however, need to be verified because they suggest climate parameters which, throughout this period (from ~60,000 to ~30,000 yr BP), are either fluctuating (Les Echets) or poorly marked (La Grande Pile).

Because of differences in the sediments, it is difficult to compare results for the two sites for the Upper Pleniglacial. Climate, during this period, was chiefly characterized by continuous low temperatures, no such equivalent being found since the beginning of the Eemian.

Low-amplitude oscillations, mainly in relation to moisture, are recorded repeatedly, especially at Les Echets, but on the strength of botanical and sedimentological data, they are believed to result from local fluctuations rather than regional general climate variations¹⁷.

The Younger Dryas is not present in the available record of La Grande Pile and is poorly marked in the Les Echets/Hière-sur-Amby succession.

Implications

If one agrees with Ruddiman and McIntyre¹⁸ that an accumulation of continental ice implies a cold and humid continent, as opposed to a hot Atlantic Ocean between latitudes 50° and

60° N, the results presented here suggest that there were three major ice-accretion periods in Europe.

The first corresponds to the very humid and markedly cold climate of the final part of the Eemian, a prelude to the even colder and dry Melisey I stadial. The second is the end of the St-Germain I interstadial (very humid but moderately cold) which was succeeded by the cold and dry Melisey II stadial. The third ice-accretion period corresponds to the end of St-Germain II interstadial and to the beginning (markedly cold but moderately humid) of the Lower Pleniglacial, before the second very cold, dry part of this major stadial.

The main ice-accretion period, which brought about an 'inception' period¹¹ (increase of global ice above modern values), started before 110,000 yr BP, the date cited as the end of the Eemian Interglacial¹². Note that the date 115,000 yr BP corresponds to minimal insolation in June, July and August at 60° N (ref. 16). A comparison of the Earth's orbital parameters at 115,000 yr BP with those of 125,000 yr BP suggests a cooling of the soil and an increase of soil moisture¹⁹ in regions situated between the Mediterranean Sea and Siberia.

Isotopic and pollen analyses of an eastern Atlantic core have shown that the fall in the oxygen isotope curve based on benthic foraminifera—the beginning of the first ice-growth phase somewhere within polar latitudes—was contemporaneous with the expansion of *Carpinus* in Europe²⁰. However, our results suggest that in Europe, the first glacial accretion began only after the *Abies* forestation episode, which followed the *Carpinus* forestation episode. This accretion, evident in foraminifera $\delta^{18}\text{O}$

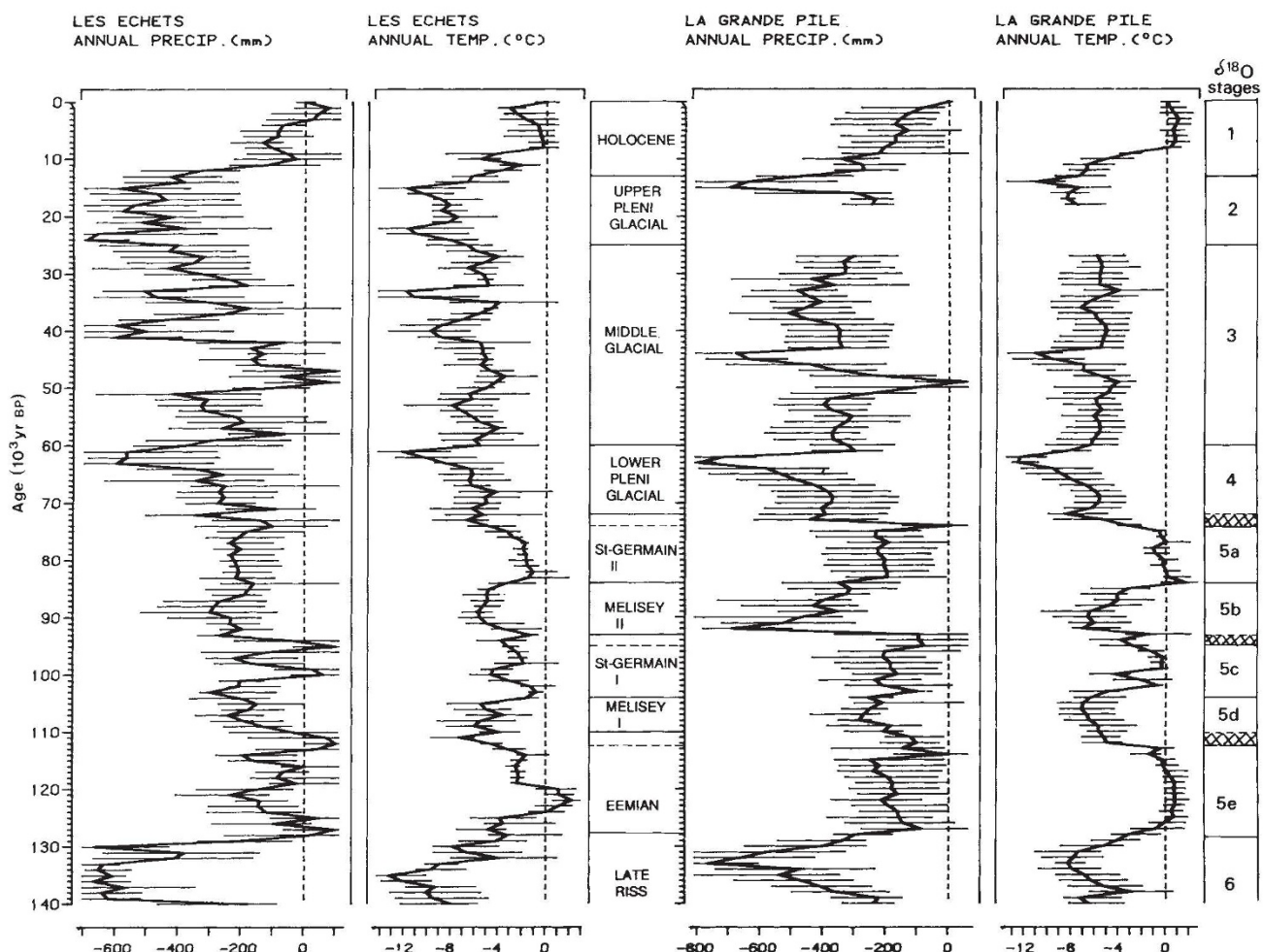


FIG. 3 Reconstruction of variations in annual total precipitation and mean temperature, expressed as deviations from the modern values (1,080 mm and 9.5 °C for La Grande Pile, 800 mm and 11 °C for Les Echets). The error

bars are computed by simulation. The vertical axis is obtained by linear interpolation from the dates indicated in Fig. 2.

data, should therefore be located in the north-west Atlantic. Changes in insolation that occurred around 115,000 yr BP and which are considered to account for this event²⁰ would then have brought about the glacial accretion on the European side of the Atlantic, with a substantial delay, as has been suggested previously²⁸. As our chronology depends on the isotopic chronology, however, we cannot say how long this delay was.

It is generally advocated (for example, refs 14 and 20) that marine isotopic stages or sub-stages characterized by low $\delta^{18}\text{O}$ values correspond exactly with stadial or pleniglacial continental episodes. Our reconstruction shows, during the first part of the last climatic cycle, well characterized transitions between periods of either low oceanic $\delta^{18}\text{O}$ values (interglacial or interstadial climatic optimums) or high ones (stadials or pleniglacial). As a result, the lower limit of the continental equivalent of isotopic sub-stages 5d and 5b and of stage 4 should be situated within transition periods and not correlated exclusively and directly with the Melisey I and Melisey II stadials or the Lower Pleniglacial, so that our results are more consistent with the interpretation of the marine isotopic stratigraphy concerning the duration of substages 5d and 5b and of the stage 4 than is the previous interpretation of the continental climatic record^{14,20}. It is

noteworthy that the transition periods, which play a major part in initiating ice-sheet formation, are forested periods. They correspond to *Picea*, *Pinus* and *Betula* forests, which mark the latter part of temperate episodes that follow the warm climate optimum; such forestation episodes are therefore often called 'post-temperate'.

The palaeobioclimatic operator appears to be the best botanical indicator of climate change, and should be preferred to the AP sum, which is unreliable, particularly for estimating palaeotemperatures. However, our reconstruction clearly suggests quite temperate conditions for the St-Germain I and St-Germain II interglacials, conditions almost similar to those of the present day, especially in relation to temperature. Such temperate phases are not recorded in the Antarctic ice cores²², in Pacific Ocean records²³, or in Atlantic Ocean deep-water temperature estimates²¹. More surprisingly, neither are they found in records from northern Europe^{24–26}. This might indicate a steeper thermal gradient for these periods than for today. By applying our method to pollen sequences from Padul (Andalusia)²⁷ on the one hand and to successions which contain records of these interstadials in northern Europe on the other, it should be possible to test this hypothesis. □

Received 29 July 1988; accepted 23 February 1989.

1. Imbrie, J. & Kipp, N.G. in *The Late Cenozoic Glacial Ages* (ed. Turekian, K.K.) 71–181 (Yale Univ. Press, New Haven, 1971).
2. Birks, H.J.B. & Birks, H.H. *Quaternary Palaeoecology* (Arnold, London, 1980).
3. Heim, J. *Les relations entre les spectres polliniques récents et la végétation actuelle en Europe Occidentale* (Université de Louvain, 1970).
4. Sabatier, R. & Van Campo, M. *Bull. Soc. bot. Fr. Actual. Bot.* **131**, 85–96 (1984).
5. Webb, T. III & Bryson, R.A. *Quat. Res.* **2**, 79–115 (1972).
6. Guiot, J. *Quat. Res.* **28**, 100–118 (1987).
7. Wollard, G. *Bull. Soc. Belge Géol.* **88**, 51–69 (1979).
8. de Beaufieu, J.L. & Reille, M. *Boreas* **13**, 111–132 (1984).
9. Clerc, J. *Doc. Cartog. ecol. Grenoble* **28**, 65–83 (1985).
10. Emiliani, C. *J. Geol.* **63**, 538–578 (1955).
11. Shackleton, N.J. *Proc. R. Soc. Lond.* **B174**, 135–154 (1969).
12. Imbrie, J. et al. *Milankovitch and Climate I* (eds Berger, A.L. et al.) 269–305 (Reidel, Dordrecht, 1984).
13. Howe, S.W. & Webb, T. III *Quat. Sci. Rev.* **2**, 17–51 (1983).
14. Wollard, G.M. & Mook, W.G. *Science* **215**, 159–161 (1982).
15. Turon, J.L. *Nature* **309**, 673–676 (1984).
16. Berger, A. *Vistas Astro.* **24**, 103–122 (1980).
17. Beaulieu, J.L. & Reille, M. *Abrupt Climatic Change* **102**, (Scripps Oceanogr. Inst. Ref. Ser., La Jolla, 1985).
18. Ruddiman, W.F. & McIntyre, A. *Science* **212**, 617–627 (1981).
19. Royer, J.F., Deque, M. & Pestaix, P. *Milankovitch and Climate II* (eds Berger, A.L. et al.) 733–763 (Reidel, Dordrecht, 1984).
20. Pufol, C. & Turon, J.L. *Bull. Ass. Fr. pour l'Etude Quat.* **1/2**, 17–25 (1986).
21. Labeyrie, L., Duplessy, J.C. & Blanc, P.L. *Nature* **327**, 477–482 (1987).
22. Jouzel, J. et al. *Nature* **329**, 403–406 (1987).
23. Shackleton, N.J., Imbrie, J. & Hall, M.A. *Earth planet. Sci. Lett.* **65**, 233–244 (1983).
24. Andersen, S.Th. *Danish Geol. Unders.* **75**, 1–175 (1961).
25. Averdieck, F.R. *Fundamenta (B)* **2**, 101–125 (1967).
26. Behre, K.E. & Lade, U. *Eisze. Gegen.* **36**, 11–36 (1986).
27. Pons, A. & Reille, M. *Palaeoclimatol. Palaeoecol.* **66**, 243–263 (1988).
28. Duplessy, J.C. et al. *Current Issues in Climate Records* (eds Ghazi, A. & Fantecki, R.) 28–44 (Reidel, Dordrecht, 1984).

ACKNOWLEDGEMENTS. We thank M. Couteaux, G. Jalut, H. Laval and M. Van Campo. The Lamont-Doherty Geological Observatory provided G. Wollard's original spectra. We thank A. Berger, J.C. Duplessy, J.J. Lowe and N. Shackleton for their valuable suggestions, Michelle Pellet for translating the manuscript into English and K. Briffa for improving it. The drawings are by C. Goeruy. This research was supported by the ECC (Climate Program) and PNEDC (Programme National d'Etude de la Dynamique du Climat).

The *Caenorhabditis elegans* heterochronic gene *lin-14* encodes a nuclear protein that forms a temporal developmental switch

Gary Ruvkun & John Giusto

Department of Molecular Biology, Massachusetts General Hospital and Department of Genetics, Harvard Medical School, Wellman 8, Massachusetts General Hospital, Boston, MA 02114, USA

During wild-type development, a protein product of the *Caenorhabditis elegans* heterochronic gene *lin-14* is localized to nuclei of specific somatic cells in embryos and early larvae, but is absent in late larvae and adult soma. Gain-of-function *lin-14* mutations cause the level of *lin-14* protein to remain high throughout development, resulting in developmental reiterations of early cell lineages. The normal down-regulation of the *lin-14* nuclear protein level encodes a temporal switch between early and late cell fates.

DURING the development of multicellular organisms, genes specify the proper developmental fates of cells in particular spatial domains^{1,2} or particular cell lineages^{3,4}; mutations in such genes transform the fates of cells into those normally found at different positions or lineages. In *C. elegans*, the temporal pattern of the cell types generated during development is explicitly controlled by heterochronic genes in an analogous manner^{5–7}. Heterochronic mutations cause particular cells in various cell lineages and tissues to adopt fates during post-embryonic development that are normally associated with cells at earlier or later stages of development. An analysis of mutations in the heterochronic gene *lin-14* has indicated that this gene plays a central role in controlling the temporal pattern of the *C. elegans* post-embryonic cell lineage^{6,7}. Loss-of-function *lin-14* alleles cause the precocious appearance, during early larval